Modeling the energy response of pn-CCDs in the 0.2–10 keV band

M. Popp[a,*], R. Hartmann[a], H. Soltau[b], L. Strüder[a], N. Meidinger[a], P. Holl[b], N. Krause[a], C. von Zanthier[b]

[a]*Max-Planck-Institut für extraterrestrische Physik, Gießenbachstr., D-85740 Garching, Germany*
[b]*KETEK GmbH, Am Isarbach 30, D-85764 Oberschleißheim, Germany*

Abstract

A simple analytical model has been developed to explain the shape of low-energy spectra taken with pn-CCDs, which are developed as imaging spectroscopic detectors for ESA's X-ray observatory satellite X-Ray Multimirror Mission (XMM). The model has been tested on experimental data taken with test devices at the German synchrotron Berliner Elektronen Speicherring für Synchrotronstrahlung (BESSY-I). It can be used to generate the response matrix function for pn-EPIC (European Photon Imaging Camera), one of the three X-ray cameras onboard XMM. First results in applying the model to polychromatic spectra are shown.

1. Introduction

The pn-CCD designed and developed at the MPI Halbleiterlabor will be used as an imaging spectroscopic detector in one of the three EPIC cameras [1] onboard the XMM satellite. XMM is ESA's large X-ray observatory, due to be launched in January 2000 [2,3]. It is sensitive to X-rays in the energy range of 0.2–10 keV. The design and fabrication of the devices are described elsewhere in these proceedings [4,5].

The device can be operated in a temperature range of -160 to -70°C, with a readout speed of up to 12.5 frames per second (12,800 pixel read per frame). The spectral response of the CCD is characterized by low electronic noise, good charge collection efficiency and a very thin entrance window [6], which results in high quantum efficiency and good spectral resolution over the whole energy band of interest. However, for low-energy photons, the resulting spectrum deviates significantly from a Gaussian shape. In order to deconvolute the astronomical spectra via a response matrix, a model for the energy response is necessary. For this purpose, a simple analytical model has been

developed that can be fitted to the spectra of monoenergetic photon irradiation, obtained during calibration measurements.

The concept of this so-called Partial Event Model is developed in the following Section 2. In Section 3, the measurements made at the synchrotron BESSY-I are described. The results of fitting the model to the spectra taken with different entrance windows are summarized in Section 4. The results of the quantum efficiency measurements are outlined in Section 5. The model parameters found are then used to compare simulations of non-monoenergetic illuminations with experimental data taken at the white light beamline at BESSY-I. This is described in Section 6, together with an astronomical example. In the last Section 7, we summarize the present state and give an outlook on future work to be done.

2. The partial event model

2.1. The radiation entrance window

The entrance window of the pn-CCD consists of a shallow p-implant in n-type bulk material in order to provide the depleting back contact of the device. The pn-junction is located at a depth of only 40 nm. The technology to produce such shallow implants is described in Ref. [6]. Applying a negative voltage to this contact yields an electric field throughout the whole depth of the dector of 300 μm, except for a shallow region within the p-doped part of the junction. The entrance window is only covered by an oxide layer of 30 nm thickness to prevent the silicon surface from degrading.

2.2. The process of charge generation

A photon with energy E_0 that reaches the detector back surface will be absorbed in a certain depth z_0 beneath the surface of the silicon (for absorption in the oxide, this depth may be negative), following the absorption law

$$N(z) = N_0 \mathrm{e}^{-\alpha(E_0)z} \tag{1}$$

with $\alpha(E_0) = \alpha_{\mathrm{Si}}(E_0)$ being the energy-dependent absorption constant for $z_0 > 0$, while for $z_0 < 0$ the absorption constant $\alpha(E_0) = \alpha_{\mathrm{SiO_2}}(E_0)$ for silicon oxide has to be inserted. For energies less than 8 keV transmission through the detector is negligible, as well as effects caused by the opposite surface (front side of the detector with shift registers). At the interaction point, a cascade-like process produces an increasing number of electrons having fewer and fewer kinetic energy, until a charge cloud with a number of electrons given by the pair creation energy w of thermalized electrons is generated. The correlation between the photon energy E_0 (in eV) and the charge generated in the Si (as number of electrons) is therefore given by

$$Q = \frac{E_0}{w}, \quad w = 3.75 \text{ eV} \quad \text{at} \quad -100^{\circ}\mathrm{C}. \tag{2}$$

The holes that are equally produced by this process are swept away by the electric field in the depleted region towards the back contact. Each electron may diffuse and drift under the influence of the electric field until it either leaves the dectector (only possible for the "hot" electrons in the early stage of the cascade process), recombines (especially at the p^+-implanted back surface) or reaches the storage area of the CCD, where it can be decteced in the next readout cycle. The loss processes cause an energy-dependent shape of the spectrum that differs significantly from a Gaussian which would be the ideal response for monoenergetic incident radiation. An example of how the spectrum looks like is given in Fig. 1.

2.3. The model for charge collection

For each individual photon that is absorbed, the loss processes mentioned above result in a different number of collected and subsequently measured electrons. Clearly, in order to obtain a spectrum, an average over many photon absorption processes is performed. Under the assumption that a photon happens to be absorbed at the depth z, we define the *collection function* $F(z)$ as follows:

$$F(z) = \frac{\text{mean number of electrons measured}}{\text{mean number of electrons generated in depth } z}. \tag{3}$$

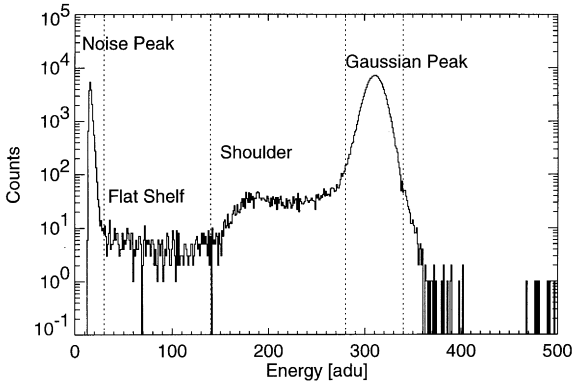

Fig. 1. A typical spectrum, taken at 1400 eV synchrotron radiation; one can well distinguish between the Gaussian part, the low-energy shoulder and the flat shelf. Due to the event threshold, the noise peak is only partially recorded and therefore not centered around 0 eV.

This function is assumed to be approximated by the following terms:

$$F(z) = \begin{cases} 0, & z \le 0 \text{ or } z \ge D, \\ S + B(z/l)^c, & 0 \le z < l, \\ 1 - A\mathrm{e}^{-(z-l)/\tau}, & l \le z < D \end{cases} \tag{4}$$

with D being the thickness of the detector (300 μm), A, B, S, c, τ, l are free parameters. A and B are eliminated under the condition of steadiness of $F(z)$ and $F'(z)$ (its derivative with respect to z) at $z = l$, leaving four free parameters.

The motivation for this functional dependence is as follows: For the ideal case that recombination is occurring only at the surface, Goto [7] has shown that the collection function is an asymptotic exponential function, as is the last term here (for $z \ge l$). The other part (for $0 \le z < l$) is motivated by the fact that the height of the shoulder in the spectra can only be reproduced by higher values of the collection function near the surface. This means that very close to the Si–SiO_2 surface, there is a region where the spacial dependence of CCE_γ is not so strong as predicted by a purely exponential model.

For $z = 0$, $F(z)$ has its minimum. The minimum number of electrons collected in the channel is therefore SE_0/w, the maximum number of electrons is $(E_0/w)F(D) = (E_0/w)(1 - A\mathrm{e}^{-(D-l)/\tau}) \simeq E_0/w$ in good approximation for typical values of the parameters. Consequently, a spectrum modeled according to this collection function shows a step-like behavior at the energy SE_0 (prior to convolution with noise). Typical value for S is about 0.5, so this step is located close to the middle between the peak and the noise peak.

Note that this collection function also reflects the effects of charge cloud size and partial reflection of thermalized electrons at the Si–SiO_2 surface, contrary to the model proposed by Lechner et al. [8,9], where the charge collection function for electrons and the charge cloud are decoupled in the first step. It should be noted that effects related to the opposite surface of the detector are not considered here, because for low and medium energies, where partial event effects are significant, the transmission of the detector is essentially zero, so that there are virtually no absorption processes close to the opposite surface, while for higher energies, where absorption is more or less uniform over the depth of the detector, absorption in either of the surface regions (a typical layer of 200 nm on each side) gives nearly no contribution to the total spectrum (about 0.1%).

Starting from Eq. (4), it is possible to calculate the resulting spectrum:

$$\frac{\mathrm{d}N}{\mathrm{d}E} = \frac{\mathrm{d}N}{\mathrm{d}z}\frac{\mathrm{d}z}{\mathrm{d}E} \tag{5}$$

where the dependence of apparent energy on the absorption depth is given by

$$E(z) := E_0 F(z).$$

Evaluation of Eq. (5) results in

$$\frac{\mathrm{d}N}{\mathrm{d}E} = \begin{cases} \dfrac{N_0 \alpha l}{cE_0 B}\left(\dfrac{B}{E/E_0 - S}\right)^{(1-1/c)} \exp\left[-\alpha l\left(\dfrac{E/E_0 - S}{B}\right)^{1/c}\right], & E_0 S \le E \le E_0(S+B), \\ \dfrac{N_0 \alpha \tau}{E_0 A^{\tau\alpha}}\mathrm{e}^{-\alpha l}\left(1 - \dfrac{E}{E_0}\right)^{\tau\alpha - 1}, & E_0(S+B) < E < E_0. \end{cases} \tag{6}$$

The noise of the system, given by the Fano-noise σ_{Fano} and the noise of the electronic readout σ_{el}, is included by convolution of Eq. (6) with Gaussian noise, given by

$$\sigma(E) = \frac{1}{\sqrt{2}\sigma_{\text{noise}}} e^{-E^2/2\sigma_{\text{noise}}^2} \tag{7}$$

$$\sigma_{\text{noise}} = \sqrt{\sigma_{\text{fano}}^2 + \sigma_{\text{el}}^2}$$

$$\sigma_{\text{fano}}^2 = 0.12 w E_0. \tag{8}$$

2.4. Modeling the flat shelf

So far, the model accounts only for events above the limit of SE_0. As can be seen in Fig. 1, there is also a small amount of events below this threshold, the so-called flat shelf. The origin of these events is the absorption of a photon near the $Si–SiO_2$ interface. Two things may happen there: either a photon is absorbed in the oxide and one or several hot electrons penetrate the interface and generate free charges in the silicon or after the absorption of a photon in the silicon, a large but arbitrary amount of energy is carried away with one or few hot electrons leaving the silicon through the interface. This should not be confused with the well-known escape peak which has a well-defined energy relation to the energy of the incident photons.

In order to account for the flat shelf, a linear collection function is assumed throughout the oxide rising from 0 to the value at the interface, S over a distance of the thickness of the oxide. Note that this is not the real physical behavior, which has a statistical nature: at an interaction point in the oxide, any amount of charge ranging from 0% to 100% may be transferred through the interface. The assumption of a linearly increasing mean averages over the different possibilities, but this simplified assumption clearly describes the observations. The calculations proceed as described above and the two parts of the spectra may be simply added together before convolution with noise is performed.

3. Measurements with synchrotron light

In fall 1996 and summer 1997 measurements with test devices were performed at the Physikalisch-Technische Bundesanstalt (PTB) laboratory at the German synchrotron facility BESSY-I. These test devices are identical with a sub-unit of the flight-type CCD. One of these devices was produced on $\langle 1\,1\,1\rangle$-material (as is the flight-type CCD) with an identical entrance window, while the other was produced on $\langle 1\,0\,0\rangle$-material for comparison reasons. At the SX-700 monochromator, a monoenergetic scan was done in the range of 200–1400 eV including quantum efficiency measurements using a calibrated PTB photodiode. In a second run, the devices were mounted in the white light beamline, where they were exposed to an undispersed 'white' synchrotron spectrum, whose spectral density distribution can be calculated from first principles [10], only relying on the energy of the electrons in the synchrotron ring and the magnetic field bending the beam. The white beam light therefore provides a possibility to calibrate the CCD without a reference photon detector. To obtain a white light spectrum the synchrotron has to be run in a special 'low-current' mode, otherwise the photon flux scaling linearly with the number of electrons in the ring would be too high. For our purposes, as few as 1–5 electrons were used as beam current.

The devices were operated at a temperature of -140°C for the $\langle 1\,0\,0\rangle$-device and -120°C in the case of the $\langle 1\,1\,1\rangle$-detector. Data were taken at a rate of approx. 10 frames per second with 12 bit energy resolution. The raw data were then processed in several steps: First, events were extracted out of the full frame signal using a 4σ discrimination threshold with respect to the noise level of the individual pixel. Next, the so-called single events were selected by discarding all events that have a neighboring event in the same frame. As a last step, the raw amplitude values of the single events were corrected for gain variations over the various readout channels and for effects of charge loss due to the transfer to the readout node. The resulting spectra were used as the database to fit the model parameters.

4. Fitting the spectra

For each spectrum, the model was fit independently using a Powell minimization algorithm on

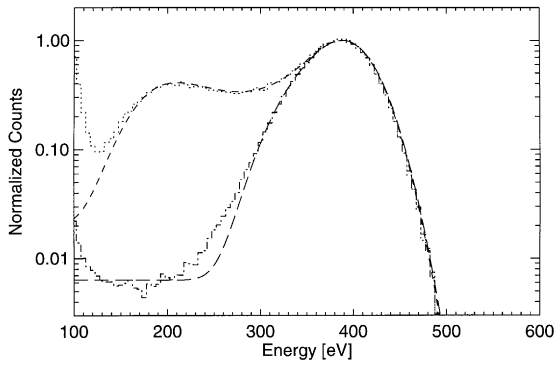

Fig. 2. Two examples of fitted spectra for different detector materials: dotted stepline: data for $\langle 1\,1\,1\rangle$-material, short dashes: model fit with parameters: $S = 0.42$, $l = 106$, $c = 1.16$, $\tau = 96$; dash–dotted stepline: $\langle 1\,0\,0\rangle$-material, long dashes: model fit with $S = 0.81$, $l = 50$, $c = 1.0$, $\tau = 93$; data were taken with a photon energy of 400 eV at the SX-700 monochromator at BESSY-I.

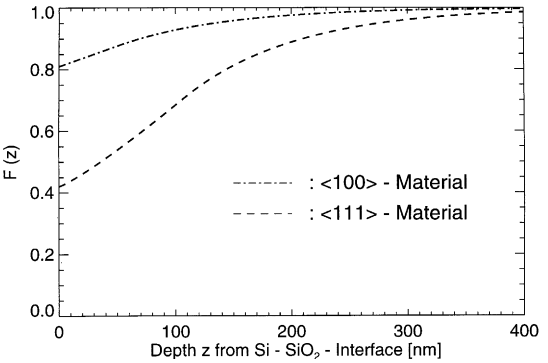

Fig. 3. Collection function for $\langle 1\,1\,1\rangle$- and $\langle 1\,0\,0\rangle$-material; the parameters are the same as in Fig. 2.

the χ^2, thus giving a set of four parameters for each energy point per CCD. As an example, two fits are shown in Fig. 2 for a photon energy of 400 eV. Note the significant difference in spectral response for $\langle 1\,1\,1\rangle$- and $\langle 1\,0\,0\rangle$-material, resulting in different best fit parameters for the two spectra. This effect has also been reported in Ref. [6].

With these parameters, one can then plot the collection function $F(z)$, see Fig. 3. It turns out that for $\langle 1\,0\,0\rangle$-material, always (except for the contribution to the shelf arising from the SiO_2–Si interface) more than 80% of the charge generated by absorption of a photon is transferred to the channel, while for $\langle 1\,1\,1\rangle$-material, near the surface only 40% of the charge is collected. This is presumably due to the higher recombination velocity at the interface for $\langle 1\,1\,1\rangle$-material compared to $\langle 1\,0\,0\rangle$-material. The parameter τ, which can be interpreted as the length scale for the transition of $F(z)$ to unity, however, is nearly the same in both cases. The reason for this is the fact that the collection not too near to the surface is governed mainly by the competing effects of diffusion of thermalized charges to the surface, where they can be lost by recombination and the drift in the electric field. The first process is isotropic and therefore independent of the orientation of the crystal, while the second is only related to the z-direction in the detector and therefore also independent of the orientation. Goto [7] has deduced an analytic solution, material constants for the ideal case of the surface layer being the only reason for charge loss. He reports a value for τ of 100 nm, in very good agreement to the value we have observed.

For a particluar CCD, only the parameter S depends on the energy of the incident photons. The parameter S determines the minimum number of electrons collected in the silicon (at $z = 0$) relative to the total number generated by the photon absorption. It is therefore an indicator for the lifetime of the electrons close to the surface. The dependence on the energy of the incident photons has been fitted on different spectra. In order to model a polychromatic spectrum for a particular CCD, only the variation of S has to be taken into account.

5. Quantum efficiency

As pointed out earlier, the quantum efficiency analysis was performed on the same data as the spectral response measurements, using in addition as a reference a calibrated photodiode together with the beam current monitor. For each energy, the flux of photons behind the monochromator was measured with the reference photodiode. Then, the CCD was put behind the aperture for a fixed time of approx. 30 min. After that, the flux was measured again. Because the flux of photons is linearly

correlated to the beam current in the synchrotron storage ring [11], the beam current monitor can be used to interpolate between the two reference measurements. For the quantum efficiency estimation, all event types (not only singles) have been selected and pile-up is accounted for. More details of the quantum efficiency analysis can be found in Ref. [12]. The results of the analysis are shown in Fig. 4. It turns out that the dependence on energy can be well described by an absorbing layer of 30 nm SiO_2 with an additional 3 nm of SiO as transition region [12]. Note that the efficiency at 200 eV is still 65%, reaching 90% close to the O–K edge at 543 eV. There the drop in efficiency is about 5%, but further analysis (not indicated in the plot) shows additional fine structure. Quantum efficiency is greater than 95% up to 9 keV, where transmission of the detector becomes important. No drop of efficiency is observed around the edge of nitrogen at 410 eV. This is due to the fact that there is no nitride deposited on the entrance window, in contrast to frontside illuminated MOS-CCDs.

6. Applications

6.1. Shift of peak positions

The model can be used to predict certain properties of the energy response of pn-CCDs, such as the dependence of the relative peak position on energy, as shown in Fig. 5. We define the relative peak position $p_{\mathrm{rel}}(E)$ as

$$p_{\mathrm{rel}}(E) = \frac{p(E)/E}{p(1400\,\mathrm{eV})/1400\,\mathrm{eV}} \tag{9}$$

where $p(E)$ is the peak position (in adu) at photon energy E. p_{rel} is then a value between 0 and 1 reflecting the deviatiation from the linear behavior. The relative peak position is constant down to 600 eV with an accuracy better than 1%. At about 400 eV, the peak position starts to deviate strongly, but this behavior is well represented by the model. So, the adu-energy scale can also be established in the nonlinear regime.

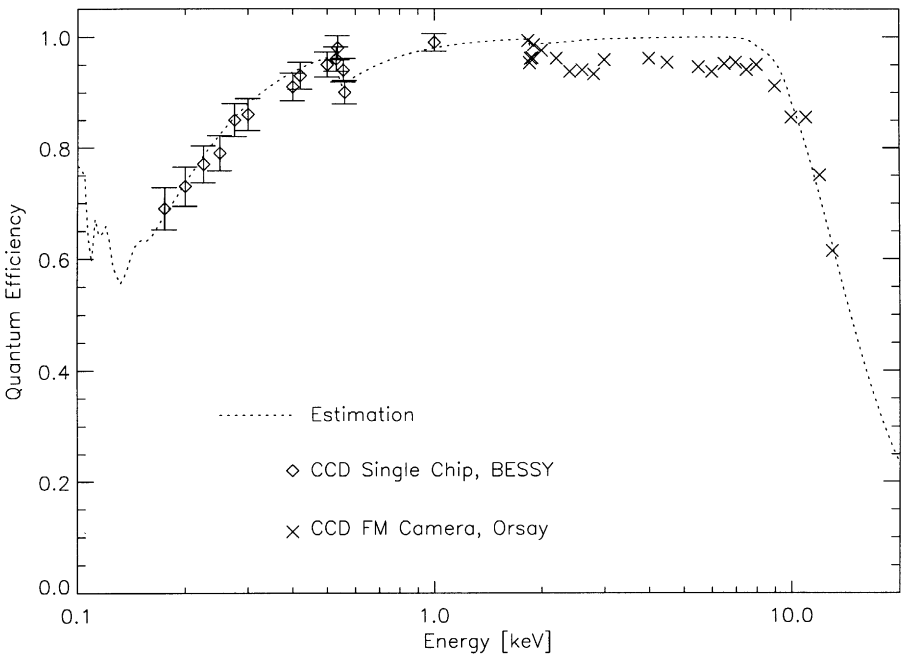

Fig. 4. Quantum efficiency of pn-CCDs measured at BESSY-I with monochromatic radiation (SX-700 monochromator), with preliminary data points for higher energies measured during the pn-EPIC flight model calibration at the Institut d'Astrophysique Spatiale (IAS) Orsay facility [12].

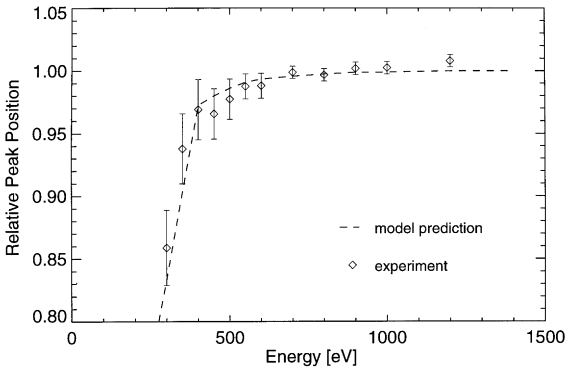

Fig. 5. Variation of peak position with energy: the relative peak positions (given in [adu/eV]) are normalized to the value at 1400 eV.

6.2. Modeling polychromatic spectra

As a test of the reliability of the model, it was applied to a spectrum generated with white synchrotron light (see Fig. 6) using the white light beamline at the PTB-Laboratory at BESSY-I. The incident spectrum follows a power law over the energy band of 100 eV to at least 10 keV. Above 6 keV, the incident photon flux is so low that only about one count per bin was recorded during the measurement. The good quantum efficiency of the device is reflected by the fact that no deviations from the steady slope are observed in the range of 1000 to 6 keV, except for a small drop at the Si-K edge at 1839 eV. The additional 'hump' just below is due to the fact that at the Si-K edge the fraction of partial events increases drastically by a factor of 20. Thus, more photons that have an energy above the edge are registered at an energy below the edge giving rise to an apparent loss of count rate just above the K-edge in conjunction with an abundance of events just below. As can be seen, this behavior is reflected by the calculated model.

For energies below 1000 eV the measured spectrum deviates significantly from the input spectrum, which is due to the fact that the quantum efficiency is not equal to one for these energies. Also, the number of partial events increases, causing a decrease of count rate at the correct energy.

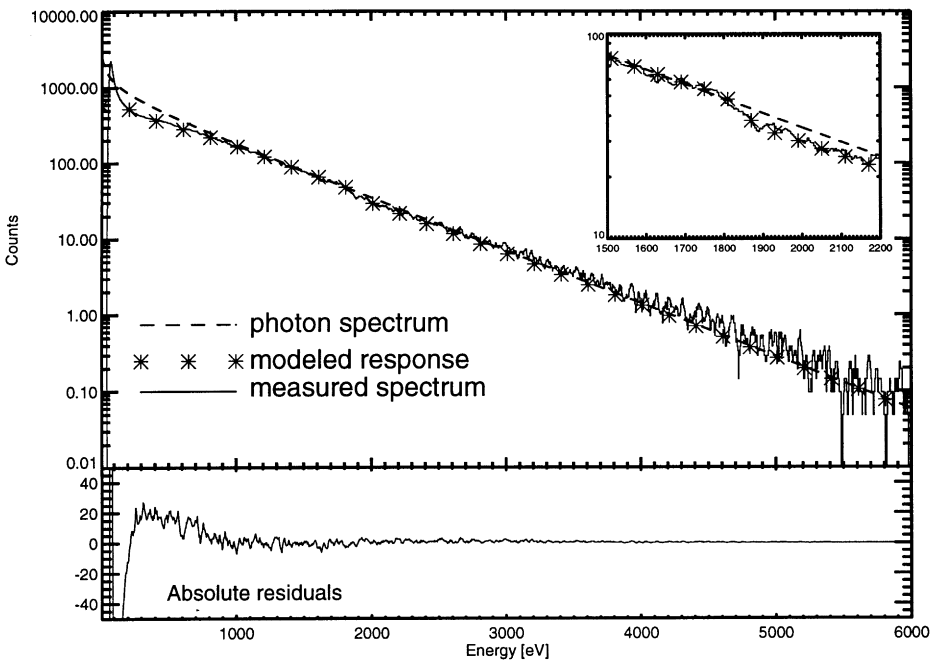

Fig. 6. Spectrum of white synchrotron light, together with the incident photon spectrum and the modeled CCD response. The inset shows details around the Si-K edge at 1839 eV.

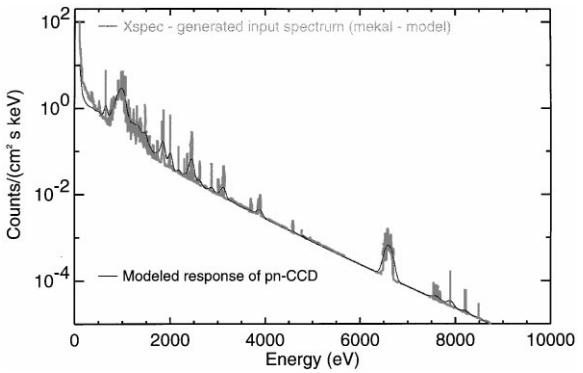

Fig. 7. As an example for a typical input spectrum, the model is applied to the simulation of an SNR (supernova remnant); neither filters nor telescope response is taken into account.

The model, in conjunction with an absorbing layer of silicon oxide, accounts for these effects with an accuracy better than 5%.

As an example for a possible application, the simulation of the response to a realistic astronomical source is shown in Fig. 7. The input spectrum has been simulated with the XSPEC software package [13], using a model for the Vela supernova remnant [14]. For this spectrum, the effects of mirrors and filters have not been taken into account. In analyzing astronomical data, the model can be used to convolute physical models of unknown sources with the detector response in order to fit parameters such as temperatures, abundances of elements, magnetic field strengths, etc.

7. Conclusions, outlook

A simple analytical model for the spectral response of pn-CCDs has been presented. This model can be adapted to different types of entrance windows by fitting the modeled response to spectra taken with a monoenergetic photon beam. Quantum efficiency can be described by assuming an absorbing layer of 30 nm SiO_2 and 3 nm SiO. The model can then be used to simulate polychromatic spectra, e.g. from white synchrotron light. One of its applications will be to generate a response matrix that will be used to extract physical parameters of astronomical sources.

This model is currently used to analyze the calibration data for the pn-EPIC flight model camera. It will be refined to account for additional features, such as split events and pile-up.

Acknowledgements

The authors are indebted to the technical staff of the semiconductor laboratory for their commitment during production of the devices and to P. Solč for bonding them. The authors wish to thank for the support provided by the PTB staff at BESSY, namely F. Scholze and R. Thornagel. This work was supported by the Heidenhain Stiftung.

References

[1] G.E. Villa et al., Proc. SPIE 2808 (1996) 402.
[2] J.F.M. van Casteren, Proc. SPIE 2808 (1996) 338.
[3] D. Lumb, H. Eggel, R. Lainé, A. Peakock, Proc. SPIE 2808 (1996) 326.
[4] N. Meidinger et al., Proc. SPIE 2808 (1996) 492.
[5] H. Soltau et al., Nucl. Instr. and Meth. A 439 (2000) 547.
[6] R. Hartmann et al., Nucl. Instr. and Meth. A 377 (1996) 191.
[7] S. Goto, Nucl. Instr. and Meth. A 333 (1993) 452.
[8] Lechner, Peter, Zur Ionisationsstatistik in Silizium, Dissertation TU München, 1997.
[9] P. Lechner, L. Strüder, Ionisation statistics in silicon X-ray detectors — new experimental results, MPE Preprint 296, 1994.
[10] T. Lederer, H. Rabus, F. Scholze, R. Thornagel, G. Ulm, Proc. SPIE 2519 (1995) 92.
[11] H. Rabus, F. Scholze, R. Thonagel, G. Ulm, Nucl. Instr. and Meth. A 377 (1996) 209.
[12] R. Hartmann, K.-H. Stephan, L. Strüder, Nucl. Instr. and Meth. A 439 (2000) 216.
[13] The XSPEC Manual http://www.rosat.mpe-garching.mpg.ge/rosat/xspec-v9.
[14] S. Holt et al., Publ. Astron. Soc. Jpn. 46 (1994) 151.